Original article

Absence of gut microbiota impairs depletion of Paneth cells but not goblet cells in germ-free *Atoh1* $^{lox/lox}$ VilCreER^{T2} mice

Mohsin Hassan [1,4 $], Oriol Juanola[2,3 $], Stefania Huber [2,3], Philipp Kellmann [4], Jakob Zimmermann[4], Edoardo Lazzarini [2], Stephanie C. Ganal-Vonarburg [4], Mercedes Gomez de Agüero[5], Sheida Moghadamrad [2,3,4]

Author's affiliations:

[1] Department of Hepatology & Gastroenterology, Charité Universitätsmedizin Berlin, 13353 Berlin, Germany.

[2] Laboratories for Translational Research, Ente Ospedaliero Cantonale, Bellinzona, Switzerland.

[3] Faculty of Biomedical Sciences, Università della Svizzera italiana, Lugano, Switzerland.

[4] Department for Biomedical Research (DBMR), University of Bern, University Clinic of Visceral Surgery and Medicine, Inselspital, Bern, Switzerland.

[5] Institute of Systems Immunology, Max Planck research group, University of Würzburg, Germany.

[$] These authors contributed equally to this work.

Correspondence:

Dr.phil.nat. Sheida Moghadamrad

Laboratories for Translational Research, Ente Ospedaliero Cantonale, Faculty of Biomedical Sciences, Università della Svizzera Italiana,

Via. Francesco Chiesa 5, 6500 Bellinzona, Switzerland

Phone: +41 58 666 71 17

E-mail: sheida.moghadamrad@usi.ch

Abstract

Mouse atonal homolog 1 (Math1/Atoh1) is a basic helix-loop-helix transcription factor important for the differentiation of secretory cells within the intestinal epithelium. The analysis of Paneth depletion efficiency upon *Math1$^{lox/lox}$VilCreER^{T2}* (*Math1$^{\Delta IEC}$*) mice treatment with Tamoxifen in the presence or absence of intestinal microbiota, showed a failure on Paneth cell depletion in germ-free mice as compared to SPF mice. However, goblet cells were efficiently depleted in *Math1$^{\Delta IEC}$* germ-free mice. The gene expression of *Math1* was significantly reduced in the ileum of germ-free *Math1$^{\Delta IEC}$* mice 5 days post tamoxifen injection as compared to germ-free control, but its protein expression was still detectable in the nuclei of epithelial cells in the crypts. Germ-free mice showed low proliferative ileal crypts as well as apoptotic cells that were mainly detected in the tip of the villus, consistent with a slow turnover rate of epithelial cells. Although Paneth cells were not depleted in germ-free *Math1$^{\Delta IEC}$* mice for the first 7 weeks after the last tamoxifen injection – far already from the 5 days timelaps observed in SPF conditions- but an incomplete depletion of Paneth cells was observed 14 weeks after last tamoxifen injection. Colonization of germ-free mice restored the phenotype observed in SPF mice, highlighting the regulatory role of gut microbes in our model. We conclude that absence of intestinal microbiota in *Math1$^{\Delta IEC}$* mice is associated with reduced epithelial cell renewal and delays the depletion of preexisting Paneth cells.

New & Noteworthy

Cre-lox system is a powerful and widely used research tool developed to understand the specific role of genes. It allows to control the spatial and temporal expression of genes in experimental models. Several limitations including toxicity of Cre recombinase or incomplete excision of floxed loci have been reported in the past. To date, this is the first research study reporting that gut microbes also influence the expected phenotype of Paneth cell-depletion in the genetically modified *Math1$^{lox/lox}$VilCreER^{T2}* mouse model.

Key words: Paneth cells; *Atoh1*; *Math1*$^{lox/lox}$*VilCreER*^{T2}; Cre recombinase; germ-free.

Introduction

The intestinal epithelium is a structure composed of a single cell layer essential for nutrient absorption, coordination of immune responses and segregation of the host from the environment (*1*). Its organization into crypt and villus compartments, together with its continuous cell renewal guarantees intestinal homeostasis (*2*). While the villi are mucosal projections to the lumen that maximize the absorptive surface area of the intestine, the crypts are formed by invaginations of the intestinal epithelium to home and protect the intestinal stem cells and ensure their proliferation (*3*). The integrity of the epithelial surface can be compromised by its constant exposure to biological and mechanical hazards. However, the stem cells located in the villus-crypt compartments guarantee a highly proliferative and self-renewing epithelium that provides protection in case of occasional breach (*4*). Paneth cells ensure an adequate sterile environment for the survival of multipotential stem cells in the intestinal crypts as they secrete antimicrobial peptides and essential niche factors (*5*).

Math1 [mouse atonal homolog 1 (*Atoh1*)] is a helix-loop-helix transcription factor that determines the cell fate of intestinal secretory progenitor cells (*6*). The depletion of Math1 results in the loss of all intestinal secretory cells including Paneth cells, goblet cell, enteroendocrine and tuft cells (*7, 8*), while its expression promotes an expansion of secretory cells associated with reduced number of absorptive enterocytes (*9*). The expression of *Math1* in the intestinal epithelium is regulated by the Notch signaling pathway since its activation represses the expression of *Math1* (*10*). The process controlling the Notch signaling in the transit amplifying compartment is known as lateral inhibition (feedback loop) that determines absorptive or secretory fate of progenitor cells by regulating the expression of *Math1* (*11*).

Genetically modified mouse models harboring Cre-lox constructions have been widely used to study the function of genes under specific spatial and temporal control (*12*). We have recently confirmed that *Math1$^{lox/lox}$VilCreER^{T2}* mice raised under specific pathogen free conditions lack secretory Paneth cells when Cre recombinase is activated with tamoxifen (*13*). Intriguingly, in the present work, we report that the depletion of goblet and Paneth cells is influenced by the intestinal microbiota in *Math1$^{lox/lox}$VilCreER^{T2} mice*.

Materials and methods

Animals

Math1$^{lox/lox}$VilCreER^{T2} colony was bred in central animal facility of University of Bern as previously reported (*13*). All animals were maintained under specific pathogen free (SPF), germ-free or ex germ-free conditions in a ventilated cage system with 12h light/dark cycle. *Math1$^{lox/lox}$VilCreER^{T2} mice* (hereafter referred as *Math1$^{\Delta IEC}$*) and Math1$^{lox/lox}$ cre negative control littermates (hereafter designated as control) were injected (intraperitoneally/subcutaneously) with 1mg/mouse/day of tamoxifen (Tm, Sigma T5648) for three consecutive days to activate the expression of *Cre* recombinase in *Math1$^{lox/lox}$VilCreER^{T2}*. Experiments were performed five days, 4 weeks, 5 weeks, 7 weeks, and 14 weeks after the last tamoxifen injection as schematically presented in Figure 1A. All animal experiments were performed according to the international regulations concerning conduct of animal experimentation. Experimental protocols were approved by research animal ethics committee of canton of Bern (authorization number BE51/20).

Germ-free rederivation from SPF Math-1 mice

As described elsewhere (*14, 15*), superovulation was performed in 3-week-old female *Math1$^{lox/lox}$VilCreER^{T2}* mice by injecting 5 IU of pregnant mare serum gonadotropin on day 0, and 5 IU of human chorionic gonadotropin on day 2. These females were paired with *Math1$^{lox/lox}$VilCreER^{T2}* males at day 2. After 2 days of pairing, the females were checked for plugs and were sacrificed to collect oviducts. The 2-cell embryos were later flushed out of the oviducts. After washing extensively, these embryos were transferred into pseudo-pregnant germ-free Swiss Webster

recipient females under aseptic conditions in the Clean Mouse Facility, University of Bern, Switzerland. Germ-free *Math1$^{lox/lox}$VilCreER^{T2}* mice were maintained after birth in flexible-film isolators in the Clean Mouse Facility, University of Bern, Switzerland with unlimited access to autoclaved food and water. Germ-free status was regularly checked by aerobic and anaerobic culturing of feces and culture-independent microscopic evaluation of SYTOX™ Green-stained fecal smears. Experimental protocols were approved by research animal ethics committee of canton of Bern (authorization number BE 1/20).

Colonization of germ-free mice

Germ-free *Math1$^{lox/lox}$VilCreER^{T2}* mice were transferred and housed in the Central Animal facility (SPF) of the University of Bern and placed in cages containing the dirty bedding and feces of the SPF *Math1$^{lox/lox}$VilCreER^{T2}* mice of the same facility and in the same rack. We colonized these mice for 8 weeks. After colonization, the mice received tamoxifen and further experiments were performed 5 days after the last injection (Figure 1B).

***Cre* and *Math1* genotyping**

Genomic DNA was isolated with the NucleoSpin DNA RapidLyse (Macherey-Nagel GmbH, Germany) from ears clips and ileum of *Math1$^{\Delta IEC}$* and cre negative control littermate mice raised under SPF, germ-free and ex-germ-free conditions. Briefly, small pieces of ear were incubated with 160 µl RLY lysis buffer and proteinase K, then incubated for 1 hour at 56 ºC on a heated shaker. Pure DNA was eluted using RLE buffer and quantified with Nanodrop. We used 10 µl of DNA (10ng/µl) for PCR to detect *Cre-recombinase* and *Math1* using specific primers: *Cre-R* (CAGGTGTTATAAGCAATCCC) and *Cre-F* (CCTGGAAAAATGCTTCTGTCCG); *Math1Lox*-R (ACACTGCTGGACACACTTGG) and *Math-1Lox*-F (CAGATCCCACAGAAGTGACG).

RNA extraction and real-time quantitative PCR gene expression

As previously reported (*16*), RNA was isolated from 30 mg of ileum preserved in RNA later (ThermoFisher) with the RNeasy Plus Mini Kit (Qiagen). We used a total amount of 0,15 µg RNA to generate cDNA by reverse transcription with the M-MLV Reverse Transcriptase (ThermoFisher). Predesigned probe and primers for *Math1*

(Atoh1) (#Mm00476035_s1, ThermoFisher) and TaqMan™ Fast Universal PCR Master Mix (ThermoFisher) were used to perform qPCR reactions in a QuantStudio™ 3 Real-Time PCR System (ThermoFisher). We used 18S rRNA (#Hs99999901_s1, ThermoFisher) as housekeeping gene to normalize the C_T values. Relative fold change values are represented ($2^{-\Delta\Delta CT}$).

Immunohistochemistry

Histologic analysis was performed as previously described (*13*). Briefly, ileum Swiss rolls were prepared and cut in sections of 5 µm. After dewaxing and rehydration of tissue samples, standard procedures were followed to block endogenous peroxidase (0.4% H_2O_2, 10 minutes), retrieval of antigens (citrate buffer, pH = 6, 15 minutes) and incubation with blocking buffer to prevent non-specific binding (TBS/1% BSA/0,1% Tween-20, 1 hour). We incubated with primary antibodies anti-Lysozyme (1:500, # PA5-16668, ThermoFisher), anti-Atoh1 (1:400, #21215-1-AP, Proteintech), anti-cleaved caspase-3 (1:400, #9664, CellSignaling) and anti-Ki67 (1:500, #ab16667, Abcam) overnight at 4ºC, followed by incubation with polyclonal goat-anti rabbit biotinylated secondary antibody (1:300, #E0433, Dako) 1 hour at room temperature. The signal was obtained after incubation with streptavidin horseradish peroxidase (Vector Laboratories) for 30 min and incubation with the substrate DAB (Vector Laboratories). We then counterstained the samples with hematoxylin (Diapath). Negative controls were not incubated with the primary antibody. Images were obtained either a panoramic digital whole slide scanner (3D HISTECH Ltd, Budapest, Hungary) or using an optic microscope coupled to a camera Axiocam ERC 5s (Zeiss) and operated by the software AxioVision Rel 4.9.1 (Zeiss). All the panels are represented at original x20 magnification. The protein expression was measured in user-defined regions of interest using a semiquantitative analysis by ImageJ software (https://rsbweb.nih.gov). The results are presented as percentage of the positively stained (brown) area in the ileal hematoxylin-stained samples.

Periodic acid-Schiff (PAS) staining

Thin ileum sections (5 µm) were deparaffinized and hydrated in water. The slides were oxidized in 0.5% periodic acid solution for 5 minutes and rinsed in distilled water. Samples were then incubated in Schiff reagent for 15 minutes to stain goblet

cells and counterstained with hematoxylin (Diapath). Goblet cells were counted, and the results were normalized to the mucosal area evaluated using ImageJ.

Statistical analysis

Statistical analyses were performed using GraphPad Prism 9 (GraphPad Software Inc., La Jolla, CA). Comparisons between two groups were performed using Mann-Whitney's U test. Data are expressed as mean ± standard deviation. P values were considered statistically significant at <0.05.

Results

In the absence of intestinal microbiota, Paneth cells are not depleted in *Math1*$^{\Delta IEC}$ mice after tamoxifen injection

As previously reported (*8, 17*), the administration of tamoxifen in *Math1*$^{lox/lox}$*VilCreER*^{T2} mice results in the activation of Cre recombinase and depletion of floxed *Math1* alleles in the intestinal epithelium (*Math1*$^{\Delta IEC}$). *Math1* is required for the differentiation of intestinal stem cells into secretory cells and for the maintenance of Paneth cells in the crypts. To confirm the loss of Paneth cells in *Math1*$^{\Delta IEC}$ mice, we evaluated in the intestinal tissue the expression of lysozyme, an antimicrobial peptide secreted by Paneth cells. As expected, Paneth cells were absent in the intestinal crypts of SPF *Math1*$^{\Delta IEC}$ mice 5 days after the last tamoxifen injection as revealed by the lack of lysozyme expression (Figure 2A). A similar immunohistochemistry analysis was performed in the group of germ-free *Math1*$^{\Delta IEC}$. In contrast to colonize mice, most of the crypts in the germ-free *Math1*$^{\Delta IEC}$ mice were positive for lysozyme indicating that Paneth cells were not depleted (Figure 2B).

Germ-free *Math1*$^{\Delta IEC}$ mice failed to show Paneth cell depletion up to 7 weeks after tamoxifen injection

It is well-known that gut microbes are essential in the intestinal development as evidenced by reduced epithelial turnover under germ-free conditions among other altered physiological parameters (*18*). Therefore, we hypothesized that 5 days after

the last tamoxifen injection may not be sufficient time for a complete depletion of Paneth cells in *Math1*$^{\Delta IEC}$ mice without intestinal microbiota. To confirm this hypothesis, we repeated the experiments in germ-free mice and harvested the intestinal tissues at different time points post tamoxifen injection. The expression of lysozyme in the intestinal tissues of germ-free *Math1*$^{\Delta IEC}$ mice consistently confirmed the presence of Paneth cells on 4 weeks (Figure 3A), 5 weeks (Figure 3B) and 7 weeks (Figure 3C) after the last tamoxifen injection. There were no differences in the abundance of Paneth cells in the ileum of *Math1*$^{\Delta IEC}$ mice as compared to their corresponding littermate Cre negative controls (Figure 3D).

Conventionalization of germ-free Math1$^{\Delta IEC}$ enables tamoxifen-induced depletion of Paneth cells

Given the unexpected results obtained in germ-free *Math1*$^{\Delta IEC}$ mice, we decided to colonize germ-free *Math1*$^{lox/lox}$*VilCreER*^{T2} mice by housing them in the SPF facility for 8 weeks (time required for a stage of instestinal development comparable to born and arise SPF mice (*19*). Interestingly, conventionalization of germ-free *Math1*$^{lox/lox}$*VilCreER*^{T2} mice followed by tamoxifen treatment resulted in the depletion of Paneth cells (germ-free *Math1*$^{\Delta IEC}$) as compared to the corresponding germ-free colonized control counterparts (Figure 4A&C). Similar results were observed with PAS staining to detect the mucin-producing goblet cell population. Although goblet cells were mostly absent in germ-free *Math1*$^{\Delta IEC}$ mice 5 days after the last tamoxifen injection, but they were more efficiently depleted in conventionalized *Math1*$^{\Delta IEC}$ mice (Figure 4B&D). These results confirmed the regulatory role of intestinal microbiota for depletion of the secretory cells in *Math1*$^{\Delta IEC}$ mice 5 days after the last tamoxifen injection.

To further decipher the underlying mechanisms of the results obtained in germ-free *Math1*$^{\Delta IEC}$ mice, we characterized the ileal expression of *Math1*. First we assessed the presence of *Cre* recombinase and *Math1* floxed alleles by standard PCR in SPF, germ-free and conventionalized mice to confirm the presence of *Cre-lox* system in our rederived germ-free *Math1*$^{lox/lox}$*VilCreER*^{T2} mice. All mice that were not injected with tamoxifen had the floxed *Math1* gene construction in the ileum and the

distribution of *Cre* recombinase among the offspring followed a Mendelian distribution in all conditions as expected (Figure 5A).

The activation of *Cre* recombination in *Math1*$^{\Delta IEC}$ mice leads to the depletion of *Math1* alleles in the intestinal epithelial cells. Since we found that Paneth cells are not depleted in the intestines of *Math1*$^{\Delta IEC}$ mice under germ-free conditions 5 days post tamoxifen injection, we therefore evaluated the expression levels of *Math1* in the ileum among all the groups to confirm whether its gene expression was changed. The excision of *Math1* floxed alleles induced by Cre recombination through tamoxifen treatment led to a reduction in the gene expression of *Math1* in the ileum of *Math1*$^{\Delta IEC}$ mice in all the conditions as compared to the corresponding littermate Cre negative controls (Figure 5B). Among Cre negative control animals, the gene expression of *Math1* was significantly decreased in germ-free conditions as compared to SPF. Interestingly, the conventionalization of germ-free mice partially restored its expression as compared to the SPF (Figure 5B). We performed an immunohistochemical assay to better describe the expression of Math1 in the ileal tissue of all study groups (Figure 5C&D). In control SPF mice, Math1 was mainly expressed in cells located in the intestinal crypts and along the ileal epithelium. However, 5 day post tamoxifen injection, the expression of Math1 was no longer detectable in the epithelium of SPF *Math1*$^{\Delta IEC}$ mice. The protein expression of *Math1* was significantly reduced in control germ-free mice as compared to control SPF mice, and it was mainly observed in a few cells of the ileal crypts and along the epithelium. Interestingly, after activation of Cre recombination in germ-free *Math1*$^{\Delta IEC}$ mice, we observed residual expression of Math1 in cells located in intestinal crypts, consistent with the presence of Paneth cells as demonstrated by the expression of lysozyme (Figure 4A). In addition, colonization of germ-free animals resulted in the phenotype similar to SPF conditions in both control and *Math1*$^{\Delta IEC}$ mice (Figure 5C&D).

Gut microbes influence intestinal development and homeostasis

The intestinal microbiota promotes epithelial cell proliferation along the intestinal tract (*20*), thereby promoting epithelial cell renewal and intestinal turnover. We evaluated the expression of Ki-67 by immunohistochemistry to detect proliferating

cells in the ileum of mice used in our study (Figure 6A&C). We did not observe significant differences in the rate of intestinal epithelial proliferation according to the genotype (*Math1*$^{\Delta IEC}$ vs *Cre* negative control) in any of the conditions studied. However, germ-free mice presented significantly reduced proliferation of epithelial cells in the ileum as compared to SPF mice. More importantly, colonisation of germ-free mice restored the cell proliferation ratio similar to the levels observed in SPF mice.

We also analyzed the presence of apoptotic cells by measuring the expression of cleaved caspase-3 in the ileal tissues of all study groups (Figure 6B&D). We did not observe apoptotic cells in the ileal tissues of mice with intestinal microbiota. However, the absence of gut microbes resulted in detection of apoptotic cells in control and *Math1*$^{\Delta IEC}$ mice mostly in the tip of the villus. Therefore, the low proliferative crypts in germ-free mice results in long-lasting epithelial cells in the epithelium of germ-free mice. Consequently, epithelial cells become apoptotic even before they are shed from the epithelial surface. These results suggest that the slow cell turnover in the intestines of germ-free mice may affect the renewal of Paneth cells in *Math1*$^{\Delta IEC}$ and plausibly explain why germ-free mice failed to develop the expected phenotype of Paneth cell depletion up to 7 weeks post tamoxifen injection.

Secretory lineage ablation in germ-free *Math1*$^{\Delta IEC}$ mice requires longer time periods post-tamoxifen injection

Although in colonized conditions, Paneth cell ablation was effective within 5 days, we considered that the average lifespan of Paneth cells in murine small intestine has been estimated up to 60 days (*21*), whereas the remaining epithelial cells , including goblet cells undergo a rapid cell renewal between 3 to 7 days, including goblet cells (*22*). Reduced proliferation rates observed in the intestinal crypts of germ-free mice may indicate delayed epithelial cells turnover. We therefore repeated the experiment for a longer time point post tamoxifen injections. Germ-free mice were administered tamoxifen and the tissues were collected 14 weeks later to ensure enough time to deplete preexisting Paneth cells. At this time point, most of the intestinal crypts (~80%) were devoid of Paneth cells, while some were still detected in isolated crypts of germ-free *Math1*$^{\Delta IEC}$ ileal tissues (Figure 7A&C). In addition, we observed a

complete depletion of the goblet cell population in the intestinal epithelium of *Math1$^{\Delta IEC}$* mice 14 weeks after last tamoxifen injection (Figure 7B&D). These findings suggest that the secretory lineage ablation in germ-free *Math1$^{\Delta IEC}$* mice is delayed for 98 days post tamoxifen injection as compared to 5-day depletion in SPF mice.

Discussion

In the present study we report that intestinal microbiota regulates the expected phenotype of intestinal secretory cells depletion in the inducible genetic mouse model *Math1$^{lox/lox}$VilCreER^{T2}*. We observed that rapidly renewed goblet cells are efficiently depleted in the ileum of germ-free *Math1$^{\Delta IEC}$* mice at short time points post tamoxifen injection similar to the SPF conditions, while Paneth cells require longer time due to their slow turnover rate. To the best of our knowledge, no study regarding the conditional deletion of the intestinal secretory cell lineage in germ-free *Math1$^{\Delta IEC}$* mice has been reported so far.

As an extended study of the previously performed experiments with *Math1$^{\Delta IEC}$* mice under SPF conditions (*13*), we aimed to perform a similar set of experiments on these mice under germ-free conditions. We performed experiments in the germ-free mice as per the standardized protocol established in SPF conditions by administering tamoxifen (1mg/mouse/day) intraperitoneally for 3 consecutive/alternate days. Due to the variability observed in the results, we evaluated the mice closely and observed that these mice failed to show the desired phenotype under germ-free conditions. Since germ-free mice have a large cecum, we suspected that failure of Paneth cell depletion in *Math1$^{\Delta IEC}$* germ-free mice might be a consequence of improper intraperitoneal administration of tamoxifen (methodological issue). We therefore changed the route of tamoxifen injection to the subcutaneous instead of intraperitoneal. However, we still observed an incomplete ablation of Paneth cells in germ-free *Math1$^{\Delta IEC}$* mice as before.

To assess the importance of intestinal microbiota on the depletion of Paneth cells in *Math1$^{\Delta IEC}$* mouse model, we colonized germ-free *Math1$^{lox/lox}$VilCreER^{T2}* mice for 8 weeks with bedding and feces from SPF *Math1$^{lox/lox}$VilCreER^{T2}* mice and repeated the experiments 5 days post tamoxifen injection. Conventionalization of germ-free *Math1$^{lox/lox}$VilCreER^{T2}* mice resulted in the loss of goblet and Paneth cells in the ileum *of Math1$^{\Delta IEC}$* mice. These findings were further confirmed with the loss of *Math1* gene expression in the ileum of *Math1$^{\Delta IEC}$* mice independent of the microbial presence 5 days after the last tamoxifen injection. Interestingly, we observed that basal gene and protein expression levels of *Math1* in germ-free control animals were restored by gut microbial replenishment. Our data are in line with the reduced transcriptional expression of *Math1* in the intestine of germ-free mice recently reported by Leon-Coria, *et al.* (*23*). At protein level, we detected low nuclear expression of Math1 in the ileal crypts of germ-free *Math1$^{\Delta IEC}$* mice 5 days after the last dose of tamoxifen. It is reasonable to speculate that the cells retaining the expression of Math1 in the ileal crypts of germ-free *Math1$^{\Delta IEC}$* mice are those Paneth cells that have not yet been depleted from the epithelium. These results may partly explain the less efficient depletion of Paneth and goblet cells in germ-free *Math1$^{\Delta IEC}$* mice after tamoxifen administration.

In the small intestine, stem cells located in the intestinal crypts of Lieberkühn, proliferate continuously and give rise to the different cell types of the epithelium. Progenitor cells differentiate into enterocytes, enteroendocrine, goblet and Tuft cells while migrating upward of the villus, until they reach the tip and become detached from the epithelium. Paneth cells follow a different path and migrate downward to the base of the crypts where they are intercalated with stem cells (*22*). As reported previously, the turnover rate of intestinal epithelial cells depends on signals from the microbiota (*14*). We then speculated that we detected preexisting Paneth cells 5 days post tamoxifen injection in the ileum of germ-free *Math1$^{\Delta IEC}$* as a consequence of a reduced turnover rate of intestinal epithelial cells. Thus, it might take longer time for these mice to deplete preexisting intestinal epithelial cells due to the absence of intestinal microbiota in germ-free *Math1$^{\Delta IEC}$*. We observed that ileal crypts of germ-free mice were less proliferative than in mice colonized with gut microbiota, and this was evidenced by the presence of apoptotic epithelial cells. Based on these observations, we speculated that epithelial cells reside longer in the ileum of germ-

free mice, and they become apoptotic even before they are shed from the epithelium. These results are consistent with the slower rate of intestinal cell turnover rate observed in germ-free intestines. We therefore repeated the experiments for a longer time after tamoxifen injection from five days to seven weeks. Nevertheless, we did not observe a significant reduction of Paneth cells in germ-free small intestines at any time point post tamoxifen injection.

The average intestinal epithelial cell turnover is estimated 3 to 7 days, except for the Paneth cells that undergo a slower cell renewal and they can reside in the small intestines up to 60 days (*21*). We therefore performed an additional experiment for 14 weeks (98 days) after tamoxifen injection in germ-free *Math1*$^{lox/lox}$*VilCreER*^{T2} mice. We found that rapidly renewing goblet cells were efficiently depleted in the absence of gut microbes 98 days post tamoxifen injection. Although Paneth cells could still be detected in a few crypts, but they were depleted in the majority of the ileal crypts of germ-free *Math1*$^{\Delta IEC}$ mice. It is therefore reasonable to speculate that under germ-free conditions, a longer time period after tamoxifen injection is necessary to induce almost complete depletion of intestinal secretory lineage, similar to the SPF conditions. However, we cannot exclude the possibility that other biological processes regulated by commensal microbiota may also influence this outcome. It is well known that intestinal microbiota influences several cellular processes including post-translational modifications (*24*) and proteasomal degradation (*25*) that play a role in the proper cellular function and localization of numerous proteins. Indeed, Math1 presents several conserved phosphorylation sites that could modulate its activity and ubiquitin-mediated degradation (*26*). In addition, we observed that stem cells differentiate into Paneth cells in the small intestine of germ-free mice despite the low gene expression levels of *Math1*. Whether other signaling pathways or transcriptional factors that are independent of Math1 play a role in the Paneth cell differentiation under germ-free conditions remains unclear. We therefore encourage future studies to address the importance of gut microbiota in the proper functioning of *Math1* and Paneth cell differentiation in the small intestine.

In conclusion, these results suggest that *Math1*$^{lox/lox}$*VilCreER*^{T2} is not an adequate model to study the consequences of Paneth cell depletion under germ-free conditions. Our findings suggest that the reduced intestinal epithelial cells turnover

rate as a plausible explanation for longer time points required to achieve secretory lineage ablation in germ-free *Math1*$^{\Delta IEC}$ mice (98 days instead of 5 days required in SPF conditions). However, the mechanisms of failure remain to be elucidated in more detail. Therefore, the present study outlines the relevance of gut microbiota to ensure intestinal homeostasis and raises an additional limitation in *Cre-loxP* mouse models, since intestinal microbiota can influence the achievement of an expected phenotype.

Glossary:

GF: germ-free

SPF: Specific Pathogen free

Math1: Mouse Atonal Transcription Factor 1

Math1$^{\Delta IEC}$*:* Math1$^{lox/lox}$VilCreER^{T2} after tamoxifen injection

Cre: Cre recombinase

Author's contributions:

MH: performed experiments and data acquisition and drafting of the manuscript; OJ: performed experiments, data acquisition, analysis and interpretation, statistical analysis, drafting of the manuscript; PK: performed experiments; SH: performed experiments, data acquisition; JZ: germ-free rederivation of *Math1* and critical revision of the manuscript; E Lazzarini performed IHC experiments; SGV: performed experiments, critical revision of the manuscript for important intellectual content; MGA: study concept and data interpretation, critical revision of the manuscript for important intellectual content; SM: study concept and design, data acquisition analysis and interpretation, statistical analysis, obtained funding, drafting of the manuscript, study supervision.

Acknowledgments:

We would like to thank Jorum Kirundi, Karin Stettler and Clean mouse facility staffs of University of Berne for technical supports in clean mouse facility; Prof. Giandomenica Iezzi and her team providing us the laboratory equipment and materials during the experiments. Prof. Lucio Barile for providing materials for IHC of

Ki-67 and RT-qPCR equipment. We also acknowledge Prof. Carlo Catapano and Dr. Simone Mosole for their support in microscopy imaging center.

Financial support:

This work was supported by a grant from the Novartis Foundation for Medical-Biological Research and a grant from Ente Ospedaliero Cantonale to Sheida Moghadamrad. OJ was supported by the Swiss National Science Foundation (IZSEZ0_205275). JZ was supported by the Marie Sklodowska-Curie grant 744257.

Disclosures:

The authors declare no conflict of interest.

Figure legends

Figure 1. Schematic representation of the project. (A) Tamoxifen injected germ-free mice were sacrificed 5 days, 4 weeks, 5 weeks, 7 weeks or 14 weeks after the last dose of tamoxifen injection. (B) Germ-free mice were colonized with intestinal microbiota by housing in the SPF animal house facility for 8 weeks. Colonized germ-free mice were sacrificed 5 days after the last tamoxifen injection. SPF *Math1*$^{\Delta IEC}$ mice and Cre negative control littermates were also included in the study.

Figure 2. Germ-free *Math1*$^{\Delta IEC}$ mice show no phenotype associated with loss of Paneth cells 5 days after the last tamoxifen injection. Representative images of lysozyme staining by immunohistochemistry in the ileum of *Math1*$^{\Delta IEC}$ and Cre negative control animals under (A) SPF and (B) germ-free conditions. n = 3 mice/group. Abbreviations: GF, germ-free; SPF, specific pathogen free.

Figure 3. Paneth cells are present in the ileum of germ-free *Math1*$^{\Delta IEC}$ up to 7 weeks after activation of Cre recombinase. Representative images of lysozyme immunohistochemistry staining in the ileum of germ-free *Math1*$^{\Delta IEC}$ after (A) 4 weeks, (B) 5 weeks and (C) 7 weeks post tamoxifen injection. (D) Cre negative control mice stained with lysozyme by immunohistochemistry at 7 weeks after last tamoxifen injection and (E) quantification of lysozyme positive crypts normalized to total ileal

crypts. Data are expressed as mean ± SD. n = 3 mice/group. Abbreviations: GF, germ-free; Lyz+, lysozyme positive crypts.

Figure 4. Reconstitution of gut microbiota in germ-free *Math1*$^{\Delta IEC}$ mice led to depletion of goblet and Paneth cells. Germ-free, germ-free colonized and SPF mice were injected tamoxifen and sacrificed after 5 days of the last injection. (A) Representative images of ileal sections stained with lysozyme by immunohistochemistry in the different study groups and (B) representative PAS staining to detect goblet cells in ileal tissue of study groups. (C) Quantification of positive lysozyme percentage area and (D) quantification of goblet cells normalized to the whole mucosal area. Data are expressed as mean ± SD. n = 3-5 mice/group. *p<0.05. Abbreviations: GF, germ-free; GF col, germ-free colonized SD, standard deviation, PAS, periodic acid Schiff; SPF, specific pathogen free.

Figure 5. Characterization of Math1 expression in *Math1*$^{\Delta IEC}$ mice with different gut microbial conditions. Germ-free, germ-free colonized and SPF mice were injected with tamoxifen and sacrificed after 5 days of last injected dose. (A) Genotyping for *Cre* recombinase and floxed *Math1* genes in the offspring *of Math1*$^{\Delta IEC}$ mice included in the study. The genotypes refer to the presence (+/-) or absence (-/-) of *Cre* recombinase. (B) *Math1* gene expression in the ileum of all study groups. (C) Representative images of *Math1* protein expression in ileal tissues of mice included in the study and (D) quantification analysis of *Math1* expression normalized per mucosal area. The arrows indicate epithelial cells expressing *Math1* located in the ileal crypts of germ-free *Math1*$^{\Delta IEC}$. Data are expressed as mean ± SD. n = 4 mice/group. *p<0.05. Abbreviations: GF, germ-free; SD, standard deviation, SPF, specific pathogen free.

Figure 6. Intestinal microbiota affects intestinal epithelial cell turnover. Germ-free, germ-free colonized and SPF mice were injected with tamoxifen and sacrificed 5 days after the last dose. (A) Representative images of immunohistochemistry detection of proliferative Ki-67 cells in ileum from all groups and (B) representative ileal images of cleaved caspase-3 detection by immunohistochemistry. (C) Quantification of positive Ki-67 cells area and (D) quantification of apoptotic cells per number of villi evaluated. Data are expressed as mean ± SD. n = 4 mice/group.

*p<0.05. Abbreviations: GF, germ-free; SD, standard deviation, SPF, specific pathogen free.

Figure 7. Depletion of Intestinal secretory lineage is delayed in germ-free *Math1*$^{\Delta IEC}$ mice. Germ-free *Math1*$^{\Delta IEC}$ mice were tamoxifen injected and tissues were collected 14 weeks later. (A) Representative images of lysozyme expression detected by immunohistochemistry in ileal tissues of germ-free mice and (B) representative images of PAS staining in ileal sections to detect goblet cells. (C) Quantification of positive lysozyme percentage area and (D) quantification of goblet cells per mucosal area. Data are expressed as mean ± SD. n = 4-5 mice/group. *p<0.05. Abbreviations: GF, germ-free; SD, standard deviation, PAS, periodic acid Schiff; SPF, specific pathogen free.

554 ## References

555

556 1. J. M. Allaire *et al.*, The Intestinal Epithelium: Central Coordinator of Mucosal
557 Immunity. *Trends Immunol* **39**, 677-696 (2018).
558 2. K. D. Sumigray, M. Terwilliger, T. Lechler, Morphogenesis and Compartmentalization
559 of the Intestinal Crypt. *Dev Cell* **45**, 183-197.e185 (2018).
560 3. H. Gehart, H. Clevers, Tales from the crypt: new insights into intestinal stem cells.
561 *Nat Rev Gastroenterol Hepatol* **16**, 19-34 (2019).
562 4. H. Clevers, The intestinal crypt, a prototype stem cell compartment. *Cell* **154**, 274-
563 284 (2013).
564 5. T. Sato *et al.*, Paneth cells constitute the niche for Lgr5 stem cells in intestinal crypts.
565 *Nature* **469**, 415-418 (2011).
566 6. P. Cray, B. J. Sheahan, C. M. Dekaney, Secretory Sorcery: Paneth Cell Control of
567 Intestinal Repair and Homeostasis. *Cell Mol Gastroenterol Hepatol* **12**, 1239-1250
568 (2021).
569 7. T. C. Liu *et al.*, Western diet induces Paneth cell defects through microbiome
570 alterations and farnesoid X receptor and type I interferon activation. *Cell Host*
571 *Microbe* **29**, 988-1001.e1006 (2021).
572 8. A. Durand *et al.*, Functional intestinal stem cells after Paneth cell ablation induced by
573 the loss of transcription factor Math1 (Atoh1). *Proc Natl Acad Sci U S A* **109**, 8965-
574 8970 (2012).
575 9. K. L. VanDussen, L. C. Samuelson, Mouse atonal homolog 1 directs intestinal
576 progenitors to secretory cell rather than absorptive cell fate. *Dev Biol* **346**, 215-223
577 (2010).
578 10. J. K. Heppert *et al.*, Transcriptional programmes underlying cellular identity and
579 microbial responsiveness in the intestinal epithelium. *Nat Rev Gastroenterol Hepatol*
580 **18**, 7-23 (2021).
581 11. R. Sancho, C. A. Cremona, A. Behrens, Stem cell and progenitor fate in the
582 mammalian intestine: Notch and lateral inhibition in homeostasis and disease. *EMBO*
583 *Rep* **16**, 571-581 (2015).
584 12. H. Kim, M. Kim, S. K. Im, S. Fang, Mouse Cre-LoxP system: general principles to
585 determine tissue-specific roles of target genes. *Lab Anim Res* **34**, 147-159 (2018).
586 13. M. Hassan *et al.*, Paneth cells promote angiogenesis and regulate portal
587 hypertension in response to microbial signals. *J Hepatol* **73**, 628-639 (2020).
588 14. K. Smith, K. D. McCoy, A. J. Macpherson, Use of axenic animals in studying the
589 adaptation of mammals to their commensal intestinal microbiota. *Semin Immunol*
590 **19**, 59-69 (2007).
591 15. E. Slack *et al.*, Innate and adaptive immunity cooperate flexibly to maintain host-
592 microbiota mutualism. *Science* **325**, 617-620 (2009).
593 16. O. Juanola *et al.*, Intestinal microbiota drives cholestasis-induced specific hepatic
594 gene expression patterns. *Gut Microbes* **13**, 1-20 (2021).
595 17. N. F. Shroyer *et al.*, Intestine-specific ablation of mouse atonal homolog 1 (Math1)
596 reveals a role in cellular homeostasis. *Gastroenterology* **132**, 2478-2488 (2007).
597 18. Y. Yu, L. Lu, J. Sun, E. O. Petrof, E. C. Claud, Preterm infant gut microbiota affects
598 intestinal epithelial development in a humanized microbiome gnotobiotic mouse
599 model. *Am J Physiol Gastrointest Liver Physiol* **311**, G521-532 (2016).

19. M. E. Johansson *et al.*, Normalization of Host Intestinal Mucus Layers Requires Long-Term Microbial Colonization. *Cell Host Microbe* **18**, 582-592 (2015).
20. A. Uribe, M. Alam, T. Midtvedt, B. Smedfors, E. Theodorsson, Endogenous prostaglandins and microflora modulate DNA synthesis and neuroendocrine peptides in the rat gastrointestinal tract. *Scand J Gastroenterol* **32**, 691-699 (1997).
21. H. Ireland, C. Houghton, L. Howard, D. J. Winton, Cellular inheritance of a Cre-activated reporter gene to determine Paneth cell longevity in the murine small intestine. *Dev Dyn* **233**, 1332-1336 (2005).
22. N. Barker, Adult intestinal stem cells: critical drivers of epithelial homeostasis and regeneration. *Nat Rev Mol Cell Biol* **15**, 19-33 (2014).
23. A. Leon-Coria, M. Kumar, F. Moreau, K. Chadee, Defining cooperative roles for colonic microbiota and Muc2 mucin in mediating innate host defense against Entamoeba histolytica. *PLoS Pathog* **14**, e1007466 (2018).
24. C. Reinhardt *et al.*, Tissue factor and PAR1 promote microbiota-induced intestinal vascular remodelling. *Nature* **483**, 627-631 (2012).
25. E. O. Petrof *et al.*, Probiotics inhibit nuclear factor-kappaB and induce heat shock proteins in colonic epithelial cells through proteasome inhibition. *Gastroenterology* **127**, 1474-1487 (2004).
26. J. Mulvaney, A. Dabdoub, Atoh1, an essential transcription factor in neurogenesis and intestinal and inner ear development: function, regulation, and context dependency. *J Assoc Res Otolaryngol* **13**, 281-293 (2012).

Figure 1

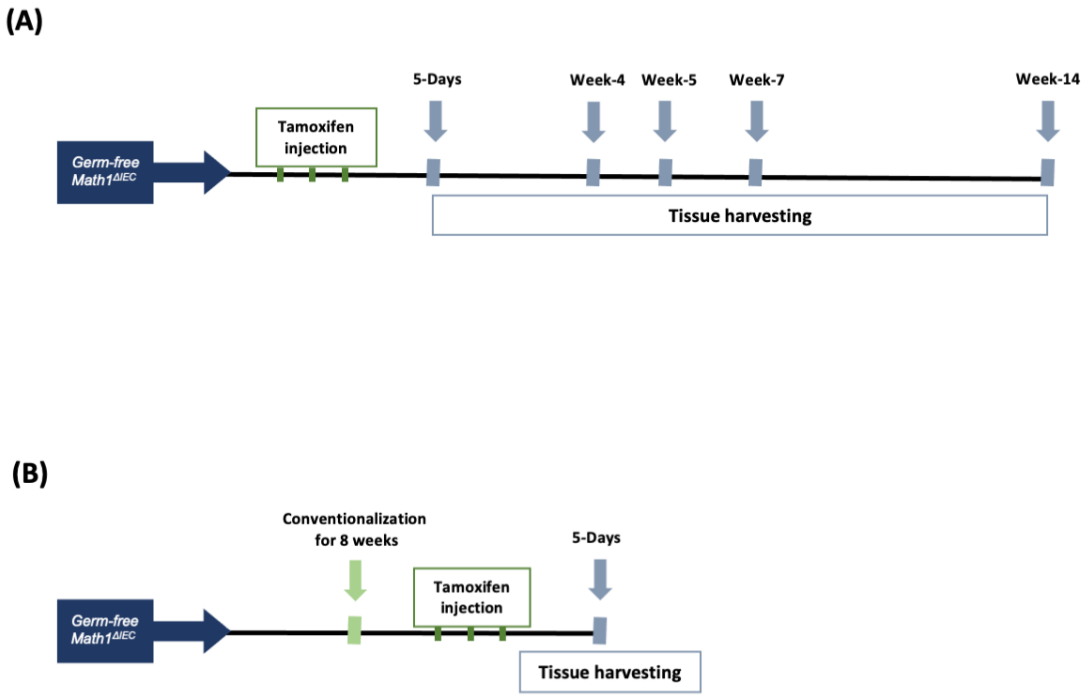

Figure 2

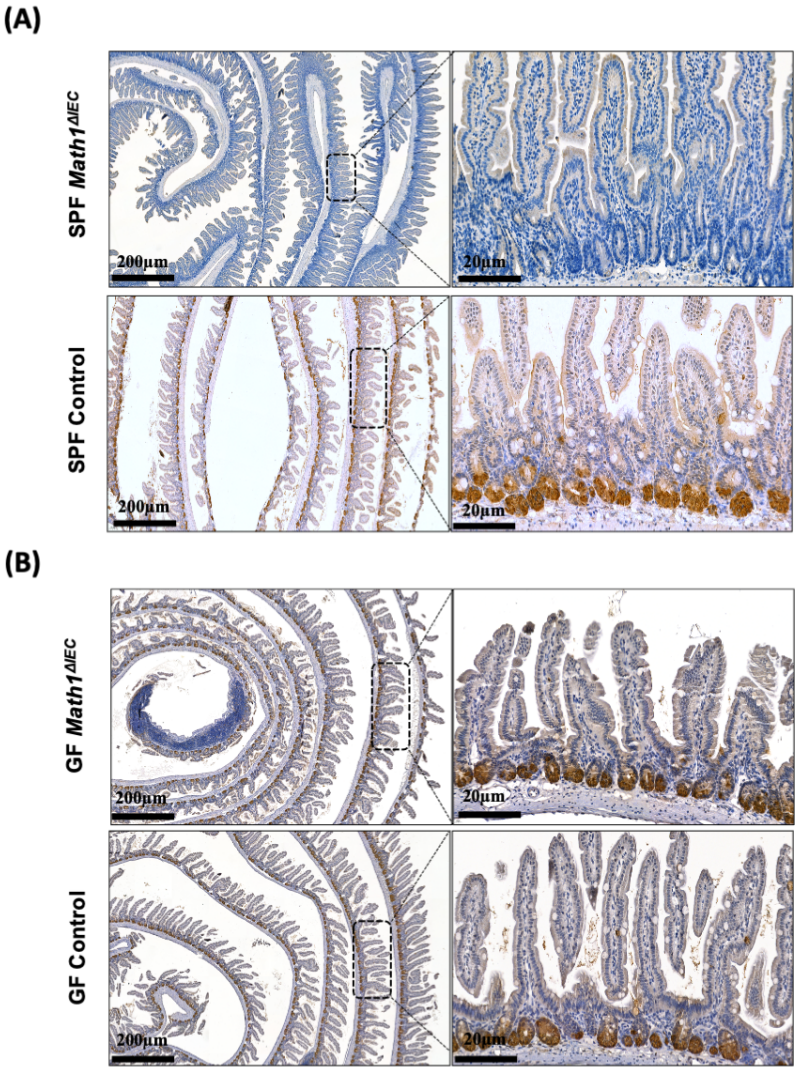

Figure 3

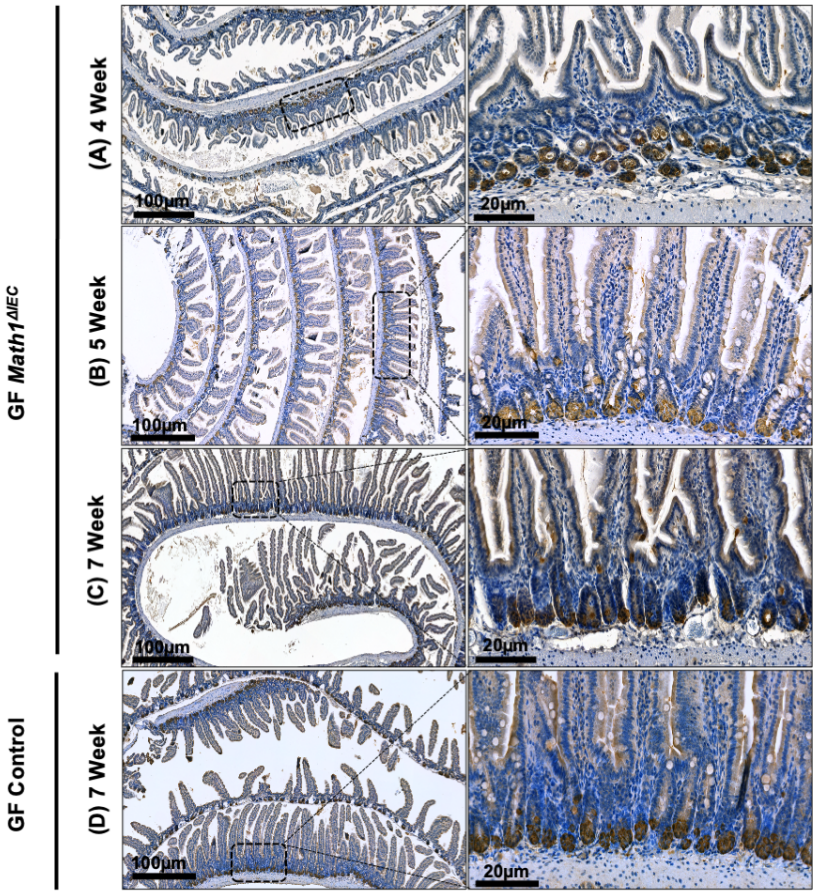

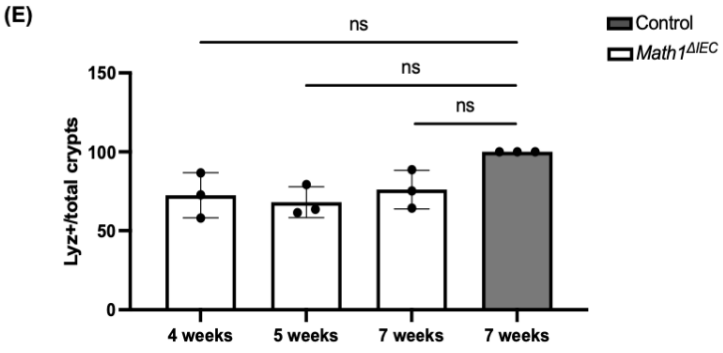

Figure 4

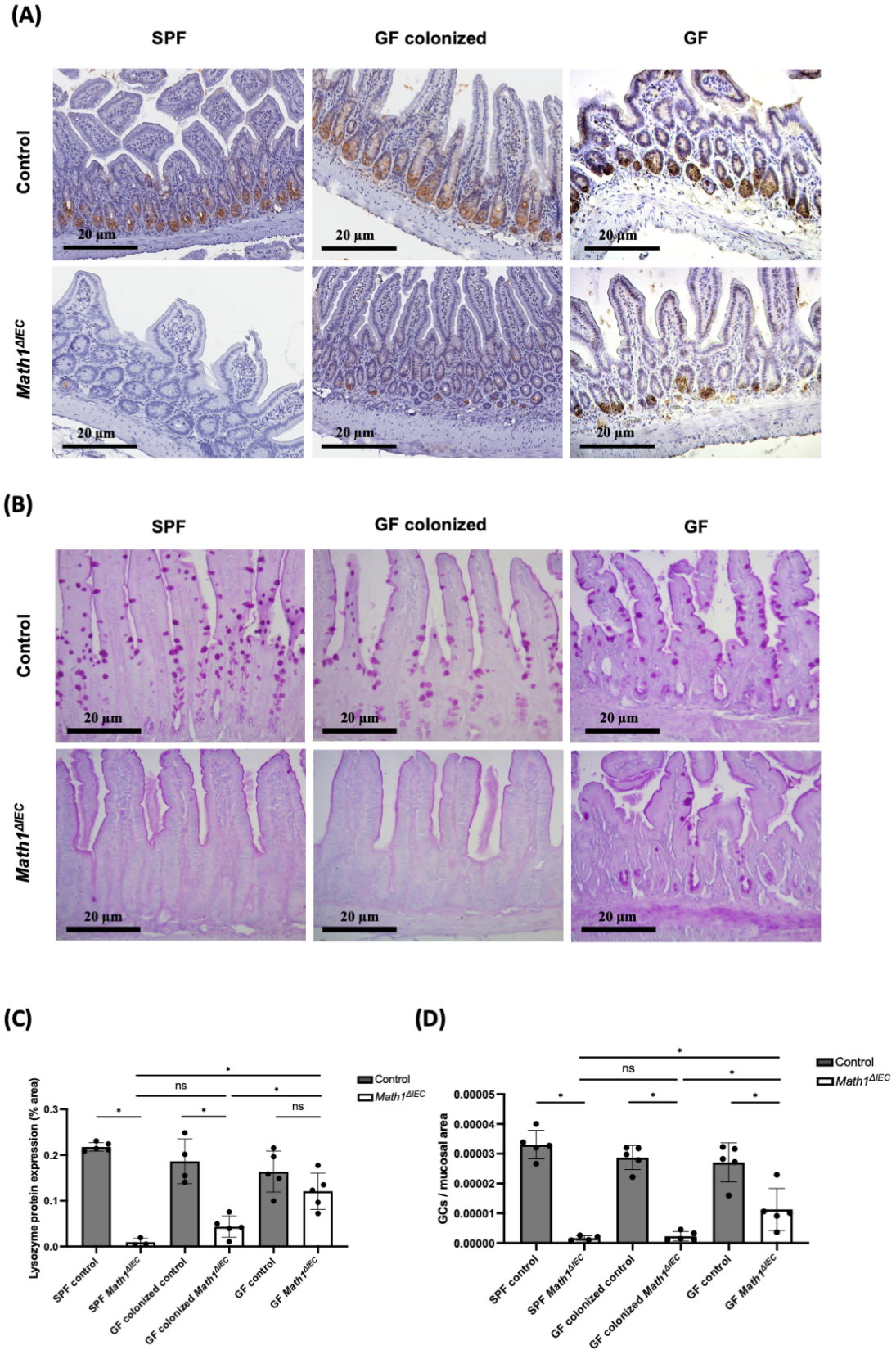

Figure 5

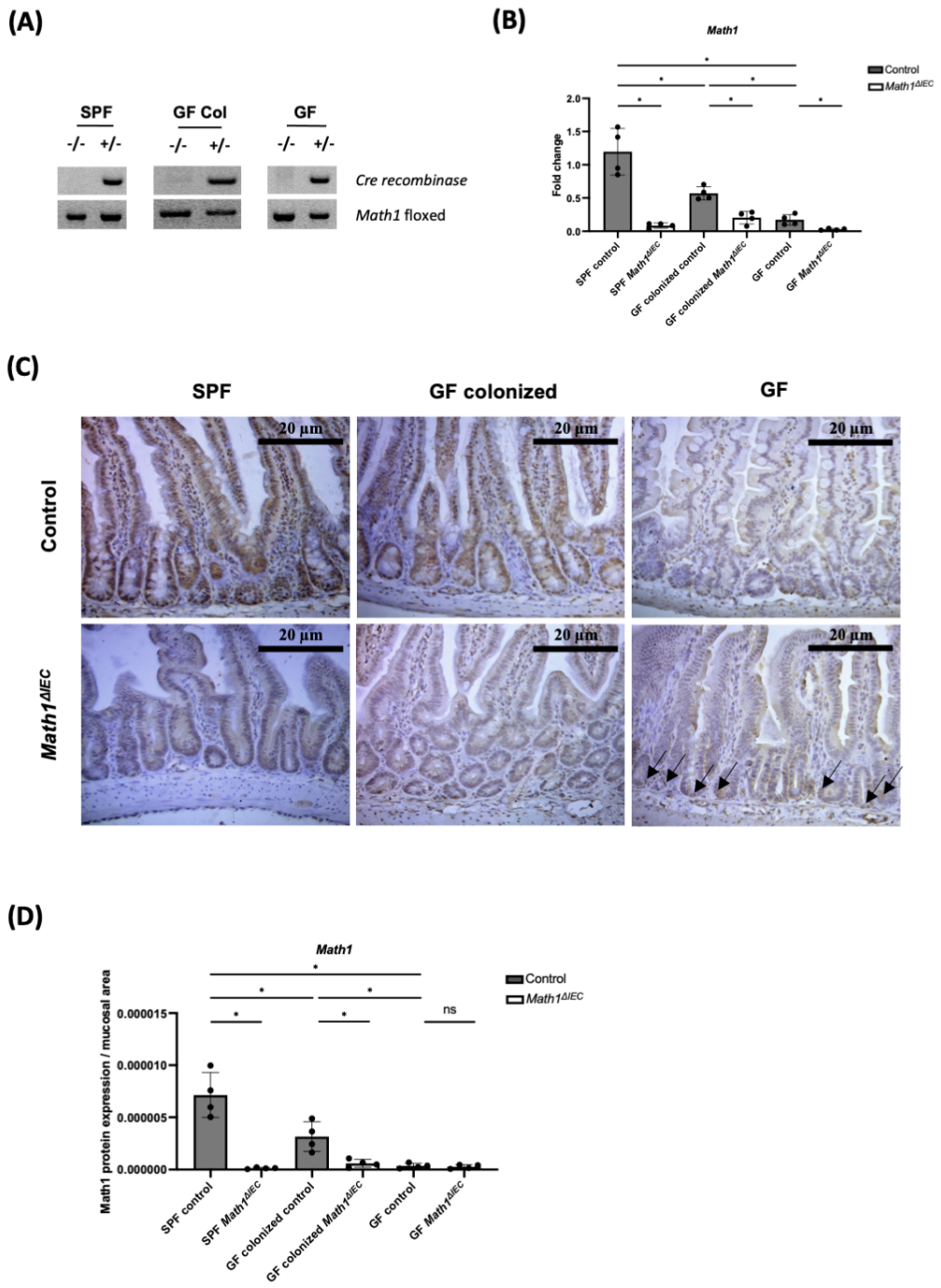

Figure 6

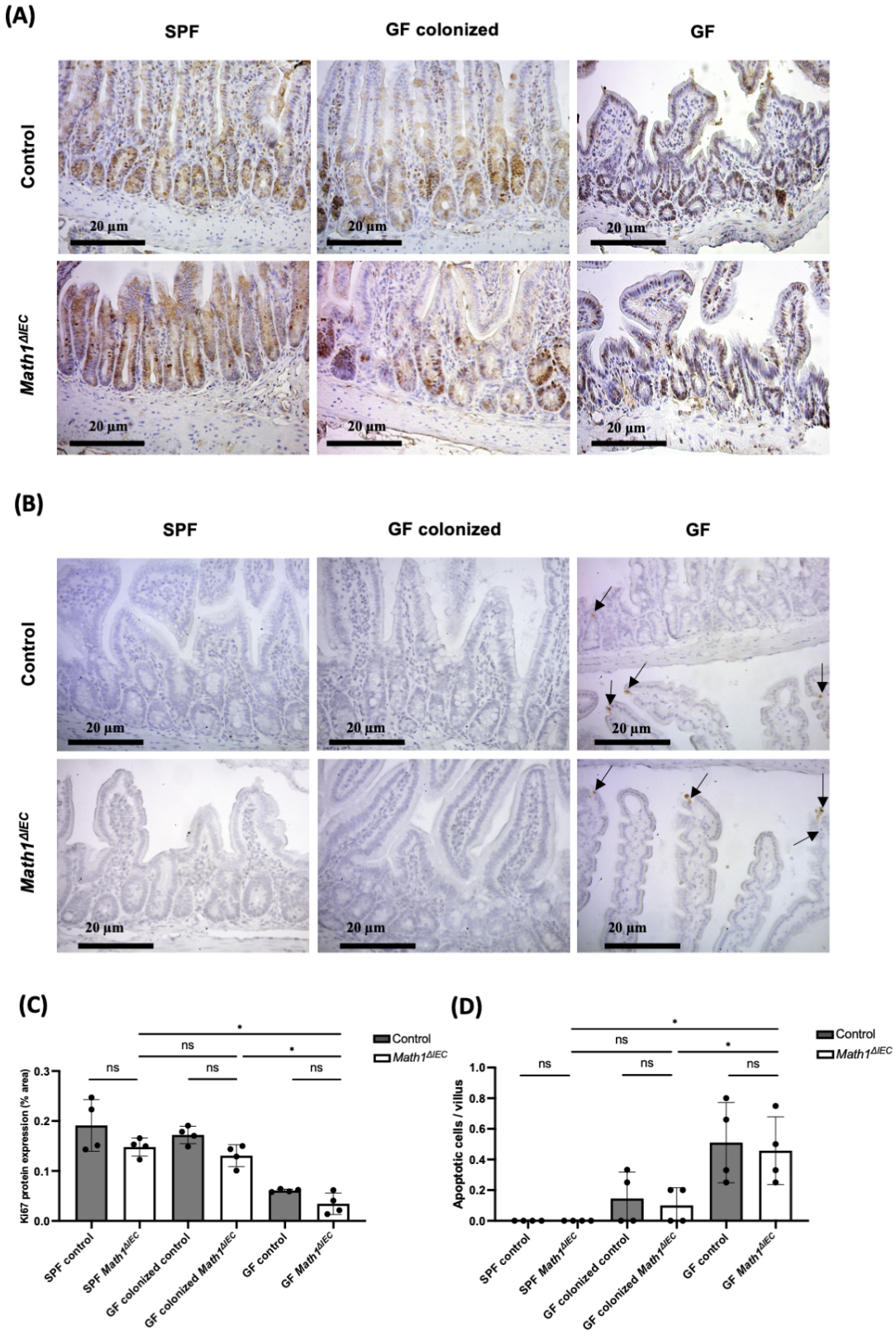

Figure 7

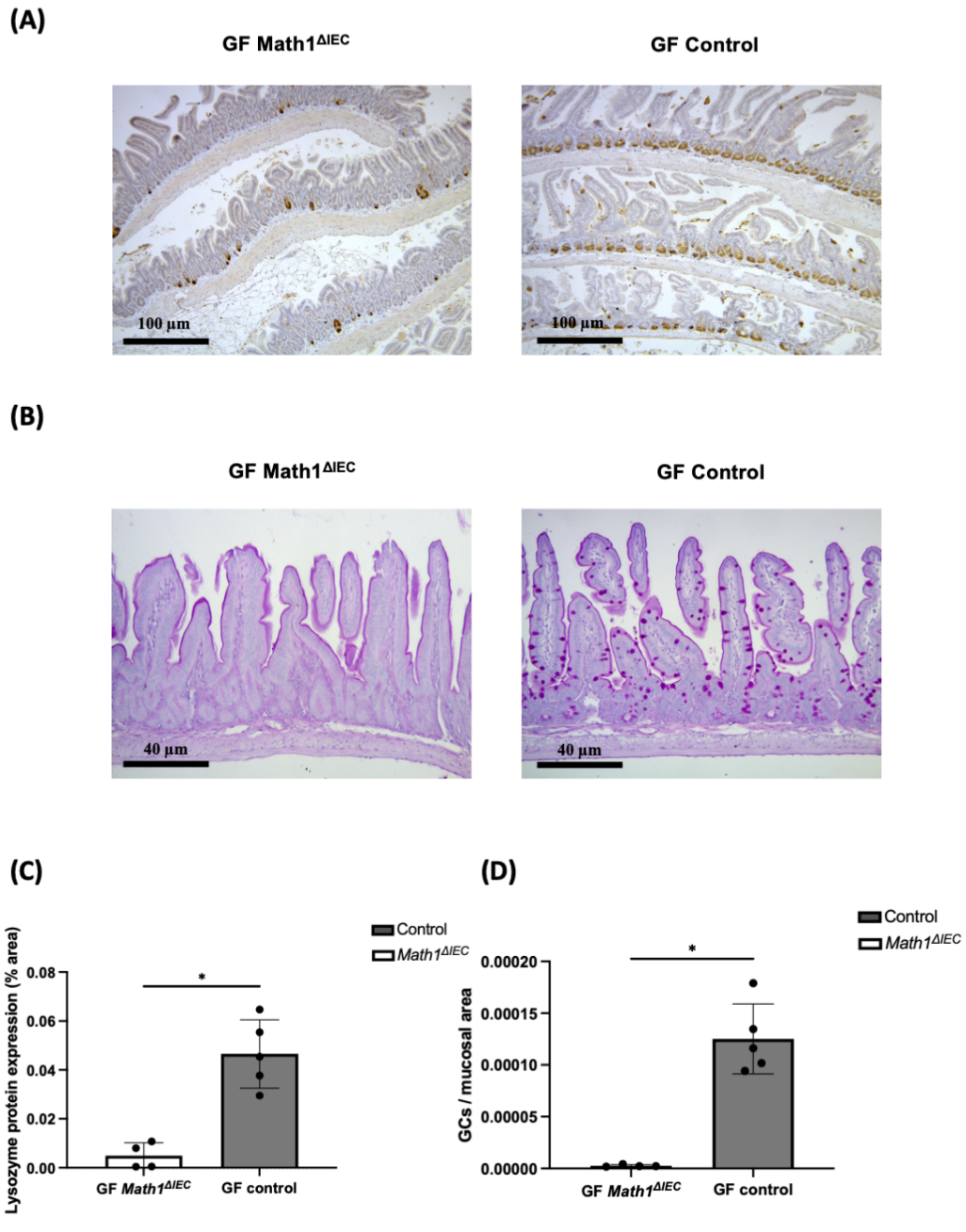

Absence of gut microbiota impairs depletion of Paneth cells but not goblet cells in germ-free *Atoh1* $^{lox/lox}$ VilCreER^{T2} mice